Discover Applied Sciences

Research

PLA-HA/Fe_3O_4 magnetic nanoparticles loaded with curcumin: physicochemical characterization and toxicity evaluation in HCT116 colorectal cancer cells

Shima Bourang[1,2] · Sina Asadian[1] · Mehran Noruzpour[2] · Atefeh Mansuryar[1] · Solmaz Azizi[2] · Hossein Ali Ebrahimi[1] · Vahid Amani Hooshyar[3]

Received: 12 December 2023 / Accepted: 26 March 2024
Published online: 03 April 2024

Abstract
Colorectal cancer (CRC) is the third most common, harmful, and universal cancer and the second lethal type. This paper discusses the therapeutic potential of curcumin, a significant curcuminoid found in the substructure of plant *Curcuma longa* (turmeric), against CRC. Curcumin has the ability to disrupt a variety of cellular signaling pathways and has been validated in several preclinical and clinical studies, but suffers from low solubility and bioavailability. Despite the widespread use of curcumin (CU) against colorectal cancer, it presents limitations, such as low solubility and bioavailability. Due to these drawbacks, researchers focused on new methods to carry CU into cells to overcome the limits of treatments with CU. One of the leading solutions is bioanalytical methods, which are based on using CU in combination with nanoparticles, especially magnetic nanoparticles, which cause the targeted transfer of the drug to cancer cells. To address these issues, PLA-HA/Fe_3O_4 magnetic nanoparticles were synthesized and loaded with curcumin. The average size and zeta potential of the nanoparticles and the magnetic properties were measured. The drug encapsulation efficiency and cumulative release of curcumin from the nanoparticles under acidic and neutral pH (4.8, 6, and 7.4) values were evaluated, as well as the cytotoxic effect of the nanoparticles on HCT116 colorectal cancer cells. According to the results of DLS and TEM analysis, PLA/Fe_3O_4/curcumin nanoparticles had a spherical structure with an average size of 208 Å ± 12.8 nm and a Zeta potential of − 18 (mV). The drug encapsulation efficiency in PLA-HA/Fe_3O_4 nanoparticles was 24.8 ± 4.6 percent. The drug's release rate was influenced by acidic and neutral pH levels. After 14 days, the highest release rate was 98% at pH 4.8 and over 94% at pH 6 (typical of cancer cells). In contrast, the drug's release at pH 7.4 (typical of healthy cells) after 14 days was only 59%. The results demonstrated that nanoparticles have a high degree of biocompatibility and the ability to carry Curcumin medications. HCT116 cells with 200 µg/ml PLA-HA/Fe_3O_4/Curcumin nanoparticles have 58.63 ± 3.7% percent cell viability. Ultimately, PLA-HA, Fe_3O_4, and Curcumin's physicochemical characteristics and impact on cell viability render them valuable instruments for precisely delivering drugs to colorectal cancer cells. The PLA-HA/Fe_3O_4–curcumin nanoparticles demonstrated a well-targeted drug delivery system for upcoming colorectal cancer treatments, as evidenced by their strong cytotoxic effects on colorectal cancer cells and negligible toxicity towards non-cancerous cells.

✉ Hossein Ali Ebrahimi, haliebrahimi@gmail.com | [1]Department of Pharmaceutics, School of Pharmacy, Ardabil University of Medical Sciences, Ardabil, Iran. [2]Department of Agronomy and Plant Breeding, Faculty of Agriculture and Natural Resources, University of Mohaghegh Ardabili, Ardabil, Iran. [3]Department of Medicinal Chemistry, School of Pharmacy, Mashhad University of Medical Sciences (MUMS), Mashhad, Iran.

Graphical abstract

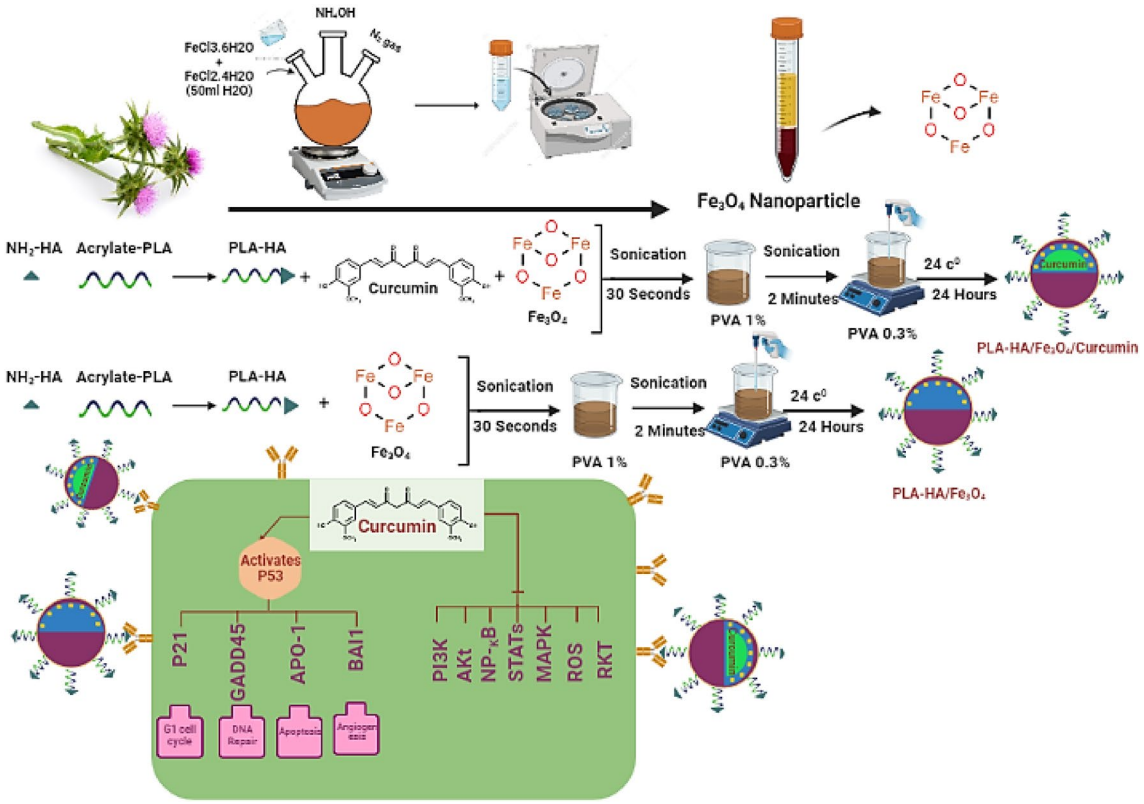

Study Highlights

- *Silybum marianum* seed methanolic extract was used as a reducing agent to synthesize NPs.
- Innovative PLA-HA/Fe_3O_4–curcumin nanoparticles show promising potential as a targeted drug delivery system for colorectal cancer treatment.
- These nanoparticles exhibit high drug encapsulation efficiency, controlled release at acidic pH levels typical of cancer cells, and significant cytotoxic effects on colorectal cancer cells while maintaining biocompatibility and minimal toxicity towards healthy cells.
- This novel approach addresses the limitations of curcumin therapy and offers a valuable tool for precise drug delivery in colorectal cancer treatment.

Keywords Curcumin · Targeted drug delivery · Nanoparticles · Green synthesis · Metastatic disease · CD44

1 Introduction

Colorectal cancer (CRC) is the third most common, harmful, and universal cancer and the second lethal type. In 2020, an estimated 1,880,725 people were diagnosed with colon cancer. By 2035, there may be nearly 2.5 million new cases [1]. According to the pathological characteristics of the tumor, there are various therapeutic options for CRC. The principal therapeutic strategy for mCRC (Metastatic colorectal cancer) patients is palliative chemotherapy, at the same time, non-systematic therapy (such as surgery and optional radiation and ablative techniques) is optional for patients with respectable metastatic lesions to improve survival [2]. The early-stage primary disease typically requires laparoscopic surgery; cases involving metastases necessitate open surgery for tumor resection, and nonresectable cases typically

require adjuvant radiotherapy [3]. Neoadjuvant and palliative chemotherapies [4], immunotherapy [5], and tyrosine kinase inhibitor (TKI) [6] therapy are additional CRC treatments. Currently, targeted drug delivery through nanoparticles has been an emerging approach for addressing various problems associated with chemotherapeutic agents [7–9].

Curcumin (1,7-bis(4-hydroxy-3-methoxyphenyl)-1,6-heptadiene-3,5-dione), likewise alluded to as diferuloylmethane, comprises one of the significant curcuminoids existing in the substructure of plant *Curcuma longa* (turmeric) [10]. Curcumin has been practically studied for the most human diseases and is highly adequate in treating a diversity of medical conditions, including, but not limited to, cancer, arthritis, major depression, liver disease, dyslipidemia, and chronic obstructive pulmonary disease [10–14]. Curcumin has the ability to encourage a wide range of chemical reactions in living things, such as hydrolysis, enzymatic reactions, reversible and irreversible nucleophilic addition (Michael reaction), and hydrogen donation leading to oxidation [15]. Evidence demonstrates that curcumin disrupts various cellular signaling pathways by directly targeting bioactive proteins or epigenetically regulating gene expression in crucial disease-associated signaling pathways, according to mounting evidence [16, 17]. Curcumin's therapeutic potential against CRC been validated several of preclinical and clinical studies, and its effectiveness in suppressing various stages of CRC development is noteworthy [18, 19]. Despite these advantages, curcumin suffers from some limitations in drug administration. Low solubility and bioavailability are major problems of this drug. Also, the passive distribution of curcumin, as to other chemical entities, is another critical obstacle to the effective anticancer properties of this drug [20]. To improve Curcumin's absorption and delivery, nano-based formulations like cubosomes and nanocarriers have been created [21]. Curcumin's bioavailability, retention in target tissues, and cytotoxic effects against cancer cells have all improved with these formulations, demonstrating encouraging outcomes [22]. Curcumin's anticancer properties have also been shown in clinical trials for various cancers, including brain tumors, lung, breast, prostate, pancreatic, gastric, leukemia, and colorectal cancers [23]. It is common knowledge that curcumin inhibits the cell cycle and speeds up cell death concerning colorectal cancer, two factors that can help prevent the disease from spreading. According to in vitro studies on different cancer cell lines, curcumin stopped the growth of the cells by molecularly interacting with several targets, which in turn regulated several distinct signaling cascade series [24]. In line with He et al., curcumin stopped the cell cycle that was partially in the G1 phase and present in the cells, which inhibited their growth [25]. Incorporating of curcumin into nanocarriers is a promising strategy to solve the mentioned problems. Nanoparticles have many significant potentials to overcome these obstacles [26]. They could increase the solubility and dissolution profile of less soluble drugs. Also, the absorption pathway of drugs may be improved using nanocarriers. However, the most attractive capability of nanocarriers is the ability to modify drug distribution in the body [27]. Since the drug is entrapped inside the nanoparticles, they can release the drug actively, and also through interaction with different organs, and biological or cell components, the fate of the drug could be changed according to treatment goals. Numerous nanocarriers were used for this strategy and, among them, the conjugation of polymeric nanoparticles with magnetic cores is very advantageous [28].

Bioanalytical methods and biomedical applications entirely rely on magnetic nanoparticles. With bio-type specimens, they encounter less background interference, making bio-type samples' magnetic susceptibilities nearly nonexistent [29]. As a result of this benefit, biological samples can be easily accessed in the direction of the external magnetic field. Analytical tools, bioimaging, biosensors, contrast agents (CAs), hyperthermia, photoablation therapy, physical therapy applications, separation, signal markers, and targeted drug delivery (TDD) are just a few of the many biomedical applications that can now be designed into magnetic nanoparticles [30]. Iron oxide nanoparticles (IONPs) are used in most studies because of their biocompatibility, high saturation magnetization, high magnetic susceptibility, chemical stability, and innocuousness [31]. Nickel and cobalt, two examples of IONPs with high magnetic properties, are toxic and easily oxidized. Magnetite (Fe_3O_4) nanoparticles (MNPs) are by far the most commonly used IONPs in biomedical applications [32]. As a result of ion transfer from Fe^{2+} ions to Fe^{3+} ions, magnetite nanoparticles have unique electrical and magnetic properties [31]. Most biomedical MNPs have superparamagnetism properties because they are smaller than 20 nm [33]. They are also widely used in this field due to their biocompatible surface chemistry, high magnetization saturation value, narrow particle size distribution (100 nm), and superparamagnetism property compared to other magnetic IONPs (M-IONPs) [29, 30, 32]. In addition to targeting tumors using an external magnetic field, magnetite nanoparticles can also cause hyperthermia-induced apoptosis of cancer cells [34]. One of the most employed polymers for coating Fe_3O_4 is PLA which is readily oxidized and agglomerated, they are often coated with natural or synthetic polymers [35].

Polylactic acid (PLA) is a flexible polymer fermented into a carboxylic acid from sustainable agricultural waste [36–38]. The lactic acid is then polymerized using a cyclic dilactone, lactide, and ring for product modification [39]. PLA and its copolymers have been utilized to encapsulate many classes of drugs, such as hormones, proteins, and chemotherapeutic agents [40–42]. Slow degradation rate and high hydrophobicity are some disadvantages that

restrict the biomedical application of PLA [43]. On the other hand, nanoparticles can actively target tumor cells by recruiting targeting moieties that bind specifically to over-expressed receptors on cancerous cells [44]. CD44, a transmembrane glycoprotein receptor, is abundantly expressed in tumor cells and plays an essential role in tumor progression and metastasis [45]. Hyaluronic acid, a natural mucopolysaccharide found in the extracellular matrix, is a CD44 ligand recently used in tumor-targeting nanoparticle formulations. The outstanding biocompatibility, biodegradability, and hydrophilicity of hyaluronic acid make it a proper candidate for the targeted delivery of drugs and genes to tumor cells [46].

Based on information mentioned above, the prescribed treatment options demonstrate efficacy in managing cancer. However, in contemporary times, with the advancement of integrated therapeutic sciences, the conventional and conventional approaches used in the past are of minimal utility in addressing critical diseases, including cancer. Therefore, contemporary researchers primarily attribute to integrating diverse methodologies in order to enhance effectiveness and overcome the limitations imposed by different techniques. In recent times, several investigations have been conducted, focusing on using various chemotherapy medications in combination with different copolymers and nanoparticles. Despite the studies conducted, based on the investigations carried out by our team, until today there is no research on the simultaneous use of curcumin, PLA-HA copolymer, and Fe_3O_4 nano particles for colorectal cancer treatment, to enhance drug efficacy, biodegradability, water solubility, release kinetics, and targeted delivery.

The purpose of this work is to assess the physicochemical properties of curcumin-loaded PLA-HA/Fe_3O_4 MNPs and determine their level of toxicity in HCT116 colorectal cancer cells. We predict these nanoparticles will present with the suitable physicochemical characteristics to facilitate drug delivery and cause cytotoxicity in HCT116 cells.

2 Materials and methods

2.1 Materials

Poly Vinyl Alcohol (PVA) were purchased from Merck (Germany). PLA, HA, $FeCl_3{\cdot}6H_2O$, $FeCl_2{\cdot}4H_2O$, RPMI 1640, penicillin/streptomycin, FBS, and DMSO were obtained from Sigma-Aldrich (USA). The MTT solution was purchased from Atocel (Hungary) and amphotericin B was obtained from Biowest (France). Other solutions, reagents, and solvents were at analytical grade and obtained domestically.

2.2 Plant collection and methanolic extract preparation of *Silybum marianum*

In the current investigation, *Silybum marianum* plants were acquired from the suburbs of Tehran and subsequently authenticated as a species (herbarium number 514) by the Botany Division of the Iranian Biological Resource Center, located in Karaj, Iran. After thoroughly washing with distilled water, the collected plants were dried at room temperature in a shaded environment. The resulting dried seeds were then finely ground to a diameter of 0.4 mm using a blender. This powdered material was subjected to methanolic extraction, employing a procedure outlined by Warthen et al. [47]. To elaborate, 30 g of the seed powder was stirred for 1 h with 300 ml of 85% methanol in a 1000-ml flask. Subsequently, the solution was incubated at a temperature of 4 °C for 48 h, followed by an additional hour of stirring. The resulting mixture was then filtered through the Whatman No. 4 filter paper. The solvent was subsequently removed under vacuum at 40 °C using a rotary evaporator. Finally, the remaining residue was dissolved in 10 ml of methanol, thus yielding a stock solution.

2.3 Green synthesis of magnetite (Fe_3O_4) nanoparticles using the methanolic extract of *Silybum marianum*

Equal amounts of $FeCl_3$ and $FeCl_2$ (3.3 g) were dissolved separately in 50 ml of water. The reaction was initiated by mixing 15 ml of *Silybum marianum* methanolic extract, $FeCl_3$, and $FeCl_2$ solution under nitrogen gas at 80 °C for 30 min using a stirrer. Then, 60 ml of NaOH (1 mM) was added to the above solution and incubated for another 4 h under similar conditions. The nanoparticles were centrifuged (10,000 rpm for 10 min) and washed several times with phosphate buffer (PBS). The resulting iron oxide nanoparticles were then freeze-dried.

2.4 Synthesis of PLA-HA copolymer

To polymerize poly lactic acid-hyaluronic acid (PLA-HA), 2 g of NH_2–Hyaluronic acid was slowly mixed with 1 g of acrylate-PLA solutions in 20 ml chloroform. The mixture was stirred for 24 h at 50 °C. To remove impurities, the resulting product was centrifuged for half an hour at 4 °C (10,000 rpm) using equal volumes of water and methanol. The copolymer was further purified using dialysis membranes (10,000 MW), and then the PLA-HA polymer was centrifuged again under the conditions as mentioned above and freeze-dried.

2.5 Characterization of PLA-HA copolymer

H-NMR spectroscopy was carried out to investigate the structure of PLA-HA copolymer using $CDCl_3$ as the solvent (Varian Unityinova 500 NMR Spectrometer, USA). Additionally, the FTIR technique (1B-AR-010, Biotec, USA) was used for confirming the synthesis of PLA-HA synthesis. Also, the thermal stability of PLA and PLA-HA copolymer was evaluated by Thermogravimetric analysis (TGA, STA-PT1000, License, Germany) in a thermal range of 40–700 °C with a heating rate of 10 °C/min.

2.6 Synthesis of Fe_3O_4 nanoparticles coated with oleic acid

As-formed Fe_3O_4 MNPs were used for the coating procedure. The particles were well dispersed in 200 ml methanol by ultrasonication. 50 ml Oleic Acid was added while constant stirring at 80 °C. OA-Fe_3O_4 particles were filtered through the Whatman filter paper no.1, washed three times with distilled water. The OA-Fe_3O_4 particles were separated from the filter paper using acetone. The particles were dried at room temperature to evaporate all the acetone. These particles were termed as OA-Fe_3O_4 NPs [48].

2.7 Synthesis of PLA-HA/Fe_3O_4/curcumin and PLA/Fe_3O_4 nanoparticles

A solvent diffusion technique was used to prepare PLA-HA/Fe_3O_4/curcumin and PLA/Fe_3O_4 without drug nanoparticles. 5 mg of Fe_3O_4 nanoparticles coated by Oleic Acid was added to PLA-HA solutions (30 mg in 1 ml chloroform). Then, 4 mg of curcumin and 1 ml of PVA solutions (1% w/v) were added to the mixture and sonicated for another 30 s, respectively. The resulting emulsions were then collected using a syringe and slowly injected into 25 ml of PVA solution (0.3% w/v) under stirring. The final emulsion was stirred at room temperature for 24 h. The yielded nanoparticles were washed three times with centrifugation using deionized water (13,000 rpm for 1 h) and freeze-dried.

In order to prepare drug-free nanoparticles (PLA-HA/Fe_3O_4), procedure as mentioned earlier, was used either. With the difference that curcumin was not added in the loading phase.

2.8 Characterization of nanoparticles

The average size and zeta potential of PLA-HA/Fe_3O_4/curcumin and PLA/Fe_3O_4 nanoparticles were determined using dynamic light scattering (DLS, SZ100, Horiba, Japan) techniques. The morphology and size distribution of synthesized nanoparticles were investigated by TEM images (LEO906, Zeiss, Germany). The formation of magnetite nanoparticles was confirmed by FTIR and UV–Vis (Thermo Scientific, USA) spectroscopy. VSM (Vibrating Sample Magnetometer, MDKF-Co., Iran) technique was used to measure the magnetic properties of nanoparticles.

2.9 Determination of drug encapsulation efficiency of synthesized nanoparticles

To calculate the drug (curcumin) encapsulation efficiency, the supernatant of the nanoparticle's mixture was centrifuged (13,000 rpm for 1 h), and the amount of free curcumin present in the supernatant was determined using spectrophotometry at 480 nm. The measured amount was then compared with the initial amount of drug used in the loading process (4 mg), and the encapsulation efficiency was calculated by the following equation:

$$EE\% = \left(W_{\text{initial CU}} - W_{\text{free CU}} / W_{\text{initial CU}}\right)$$

2.10 Release profile of drug from nanoparticles

Since the tumor tissue has a lower pH than the normal tissue, the drug release from nanoparticles was evaluated in PBS buffer with acidic (pH = 6) and neutral (pH = 7.4) pH values. 10 mg of the PLA/Fe_3O_4/curcumin and PLA-HA/Fe_3O_4 nanoparticles were added separately to 2 ml of PBS buffer and stored at 37 °C. The nanoparticles supernatant was then collected by centrifugation (13,000 rpm for 10 min) at predetermined time intervals and nanoparticles were resuspended in 2 ml of PBS until the following collection. The amount of drug present in the supernatant was evaluated using spectrophotometry. The cumulative release percentage was then calculated using the following equation.

$$\text{Cumulative release percentage: } \frac{Dr^{t} + Dr^{t+1}}{DE}$$

Dr^t = The measured amount of drug in the supernatant at any time (t); Dr^{t+1} = The measured amount of drug in the supernatant at the time (t + 1); De = The amount of drug encapsulated in the nanoparticles.

2.11 In vitro evaluation of cytotoxicity

The HCT116 colorectal cancer cell line was used to evaluate the toxicity and drug delivery efficiency of PLA-HA/Fe_3O_4 nanoparticles. First, Human Colorectal Carcinoma cell line HCT116 cells were grown in 10% fetal bovine serum and RPMI cell media at 37 °C in 5% CO_2. The cytotoxic effect of Fucosterol alone or in combination with curcumin in colon cells was evaluated by an MTT reduction assay. For the MTT assay, 100 µl of HCT116 cells at a density of 7×10^4 cells per milliliter were transferred to 96-well plates. Then, the cells were kept in a CO_2 incubator (at 37 °C, 90% humidity, and 5% CO_2) for 24 h. The HCT116 cells were then treated with different concentrations of PLA-HA/Fe_3O_4/curcumin nanoparticle (25, 50, 75, 100, 200 µg/ml), as well as free curcumin. To evaluate the toxicity of nanoparticles, PLA-HA/Fe_3O_4 was used. The cells were exposed to each treatment for 24 h. Then, the cell viability was assessed using an MTT assay.

2.12 Statistical analysis

All experiments were conducted based on a completely randomized design (CRD) in triplicate. The experimental data were subjected to analysis of variance (ANOVA) ($p < 0.05$) and mean comparison using Duncan's Multiple Range Test (DMRT) (at $p < 0.05$). Statistical analysis was performed using IBM SPSS Ver.21 statistical software (IBM Corporation and Others, Armonk, NY, USA). The results were expressed as mean ± Standard error (SE). The graphs were produced using Microsoft Office Excel 2016.

3 Results

3.1 Characterization of PLA-HA copolymer

The H-NMR spectra of PLA and PLA-HA are presented in Fig. 1. As shown in the H-NMR spectrum of PLA, the peaks observed at 5.75 (b) and 1.72 (a) ppm were assigned to methine and methylene groups in PLA. Whereas in the H-NMR spectrum of PLA-HA, new peaks were observed at 8.19 and 3.97 ppm, which were related to the alcohol (OH) (d) and amide (NH) (c) protons present in the structure of hyaluronic acid, respectively.

The FT-IR spectra of PLA and PLA-HA copolymer shown in Fig. 2, confirms the synthesis of PLA-HA. As shown in the FT-IR spectrum of PLA, the IR bands observed at 1750 cm^{-1} and 2900–3000 cm^{-1} were related to C=O and C–H groups present in PLA. The FT-IR spectrum of PLA-HA revealed new peaks at 1596 and 3532 cm^{-1} which were respectively related to N–H and O–H bonds in hyaluronic acid. These findings can indicate the bonding of HA to PLA.

TGA analysis is mainly performed to study the thermal stability of samples, but this method can also estimate the percentage of constituents present in the sample. The TGA analysis of PLA, shown in Fig. 3, represents a severe weight loss stage, which is indicative of the purity of the PLA polymer. On the other hand, several stages of weight loss were observed in the TGA analysis of PLA-HA polymer in the temperature range of 200–250, 300–320, and 350–380 °C, which

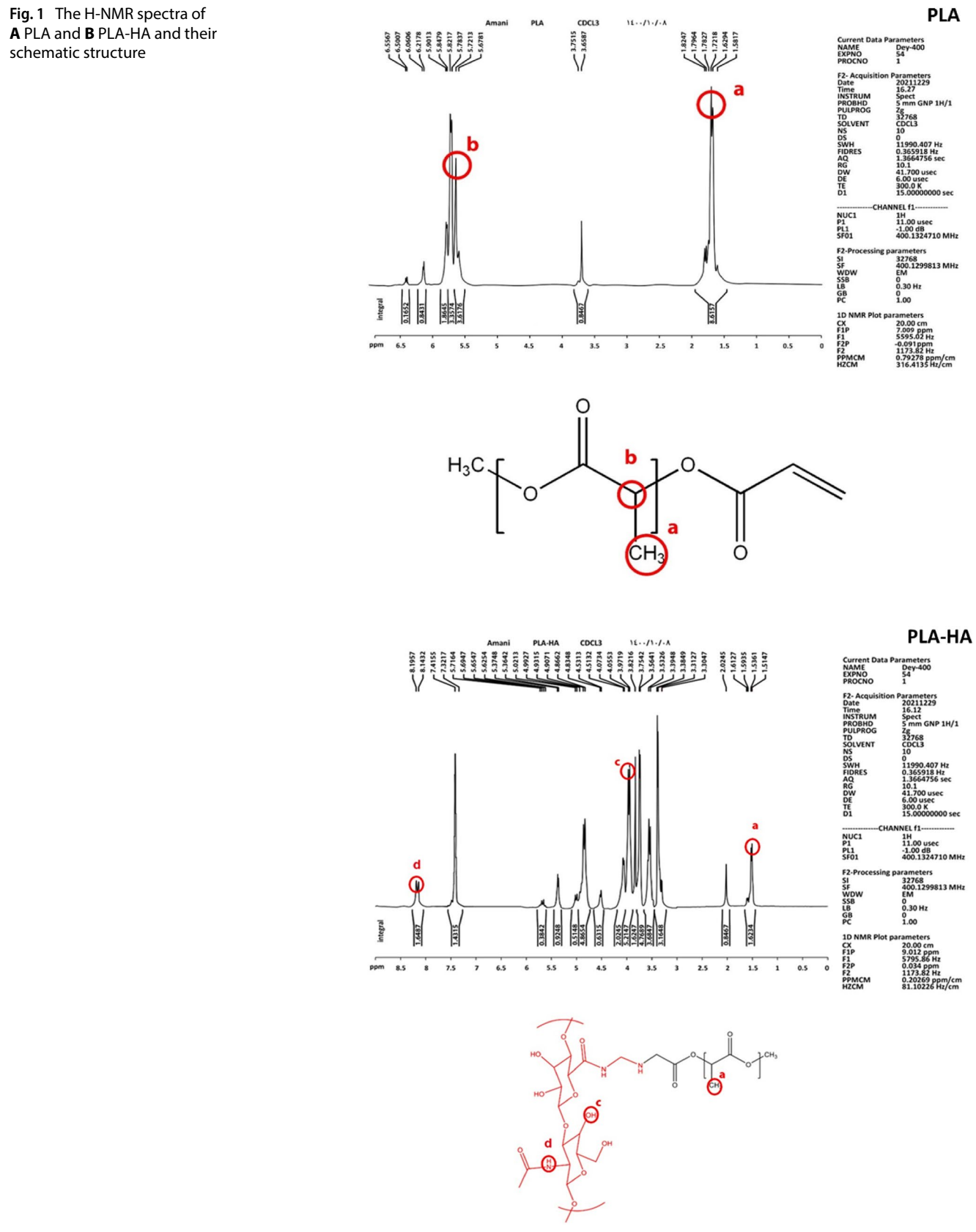

Fig. 1 The H-NMR spectra of **A** PLA and **B** PLA-HA and their schematic structure

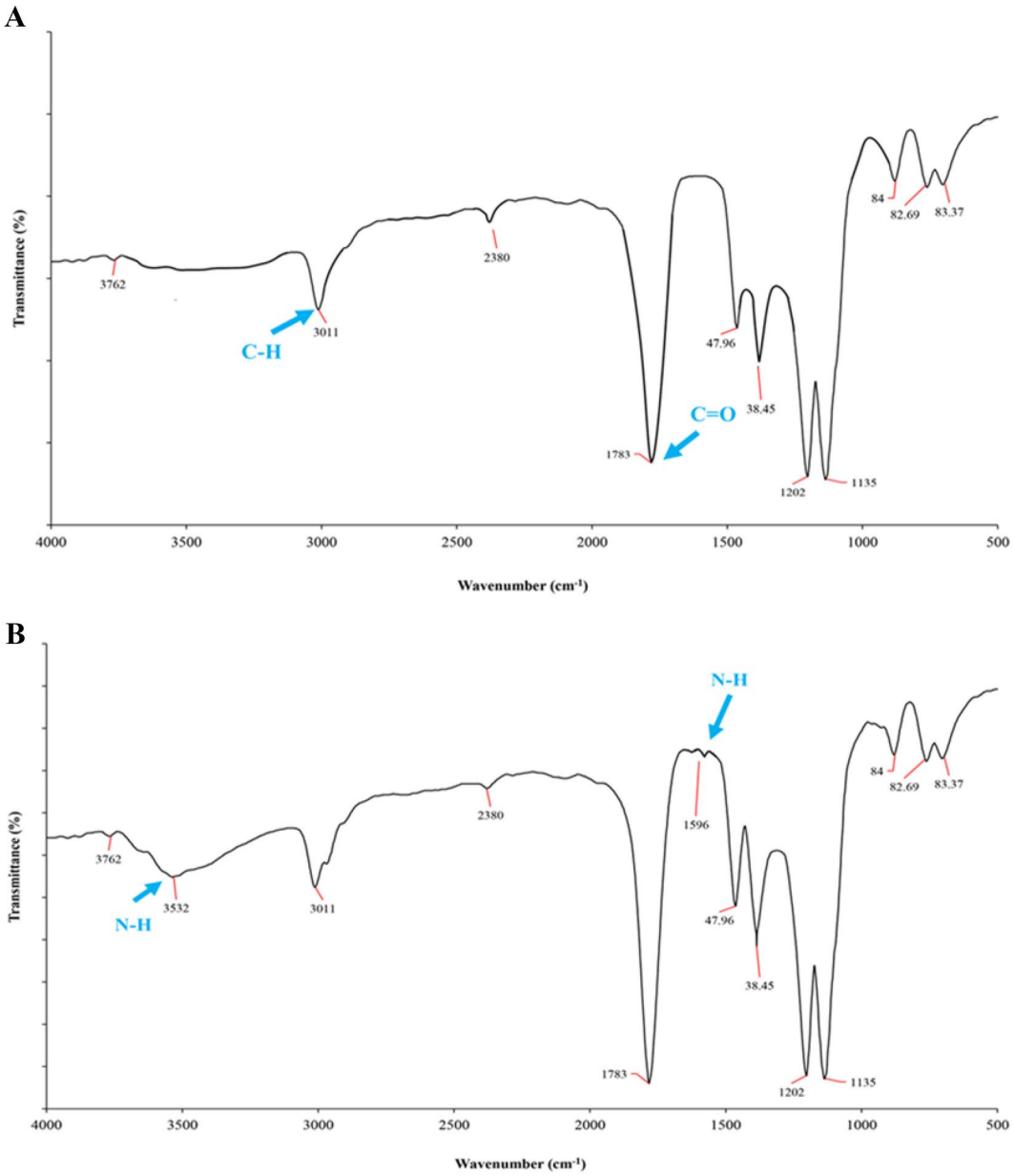

Fig. 2 The FT-IR spectra of **A** PLA and **B** PLA-HA

indicated the presence of several materials in PLA-HA compared to PLA. Considering that the weight loss of PLA was observed in the temperature range of 200–320 °C, it can be concluded that the weight loss in the temperature range of 350–380 °C is related to the hyaluronic acid present in the structure of PLA-HA copolymer.

3.2 Characterization of PLA-HA/Fe_3O_4/curcumin nanoparticles

The results of studying the morphological properties and size of PLA-HA/Fe_3O_4/curcumin nanoparticles by transmission electron microscope (TEM) indicated that these nanoparticles had a spherical structure and a size of about 100–300 nm (Fig. 4).

The DLS results shown in Fig. 5 confirm the nanoscale dimensions of the synthesized nanoparticles. According to the results, PLA-HA, PLA-HA/Fe_3O_4, and PLA-HA/Fe_3O_4/curcumin nanoparticles had an average size of 208 ± 12.8, 235 ± 8.4, and 280 ± 9.14 nm and Zeta potential of – 15, – 18, and – 17 (mV), respectively. Since the negative surface charge of the nanoparticles could be due to the negatively charged carboxylic groups present in the hyaluronic acid.

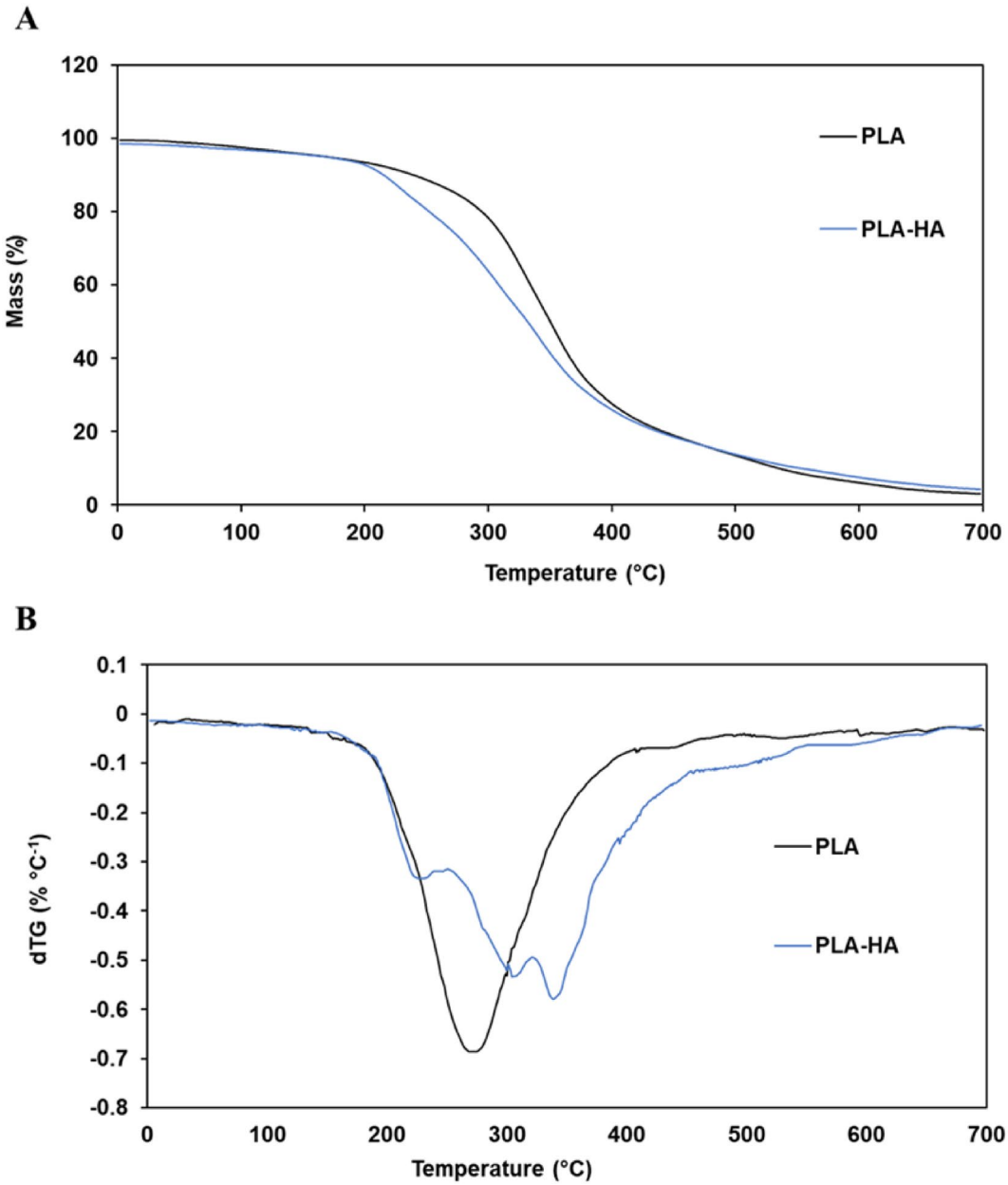

Fig. 3 **A** TGA and **B** DTG analysis of PLA and PLA-HA

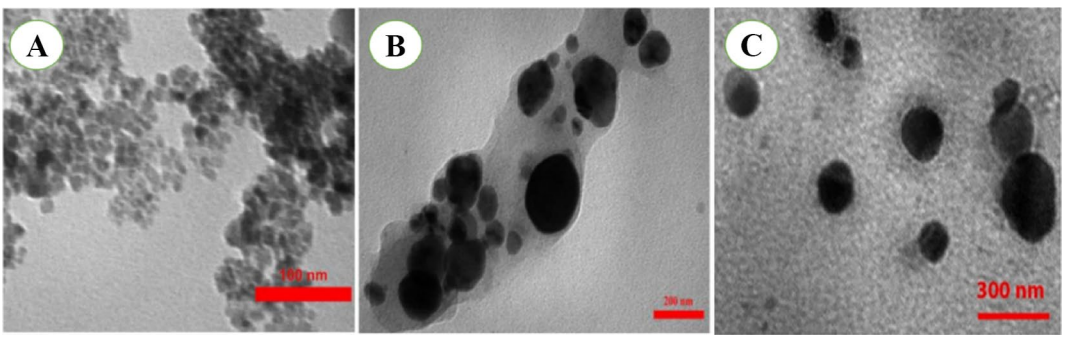

Fig. 4 TEM image of synthesized nanoparticles; **A** PLA-HA, **B** PLA-HA/Fe_3O_4, and **C** PLA-HA/Fe_3O_4/curcumin

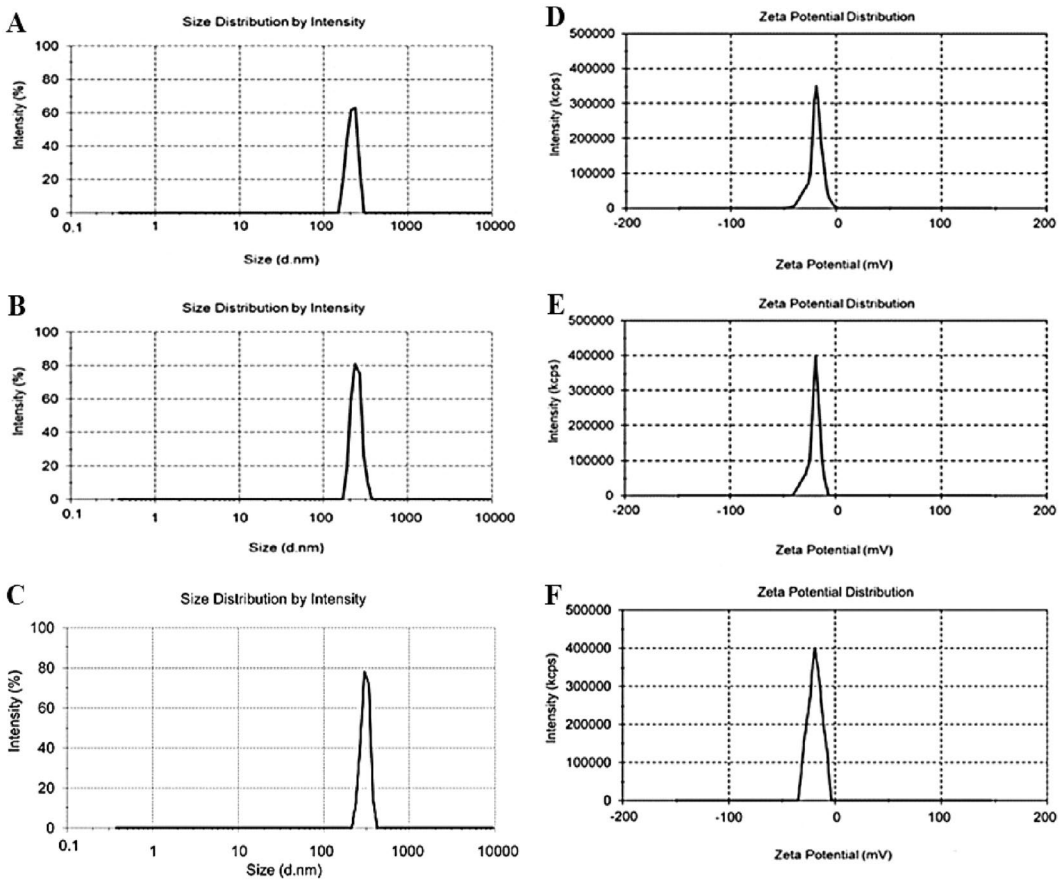

Fig. 5 DLS profile: **A**–**C** Size distribution of PLA-HA, PLA-HA/Fe_3O_4, and PLA-HA/Fe_3O_4/curcumin; **D**–**F** zeta potential analysis of PLA-HA, PLA-HA/Fe_3O_4, and PLA-HA/Fe_3O_4/curcumin

3.3 Drug release pattern

The drug encapsulation efficiency in PLA-HA/Fe_3O_4 nanoparticles was 24.8 ± 4.6%. The drug release pattern in acidic and neutral media (shown in Fig. 6) involved two different phases: burst release and sustained release. More than 50% of the drug released within 3 days was released. For example, the amount of released drug of PLA-HA/Fe_3O_4/curcumin within

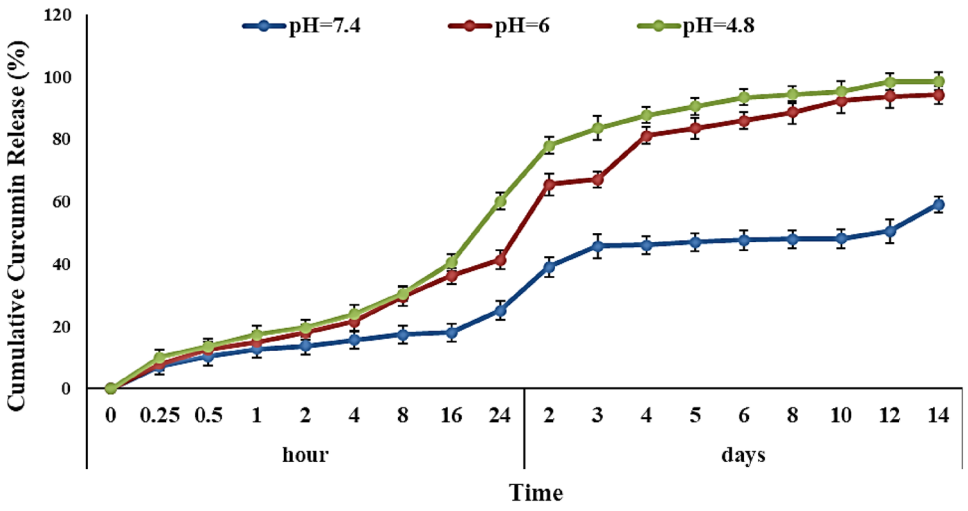

Fig. 6 Drug release profile of PLA/Fe_3O_4/curcumin nanoparticles in acidic and neutral pH (4.8, 6, and 7.4)

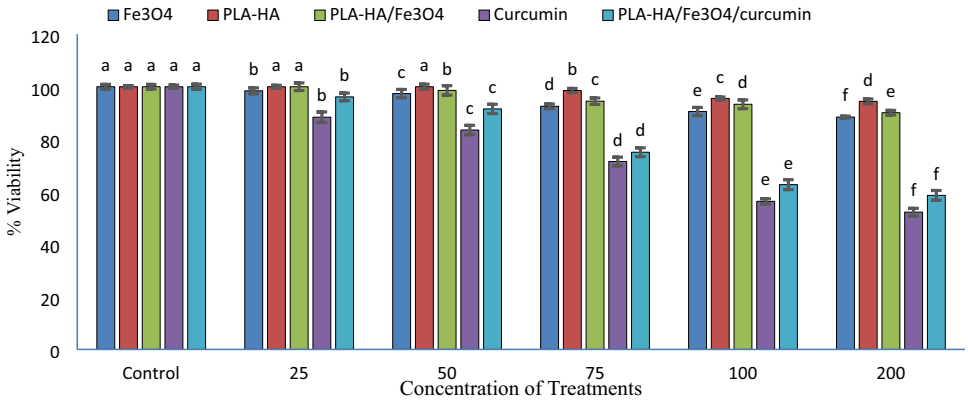

Fig. 7 Evaluation of toxicity and drug delivery efficiency of Fe_3O_4, PLA-HA, PLA-HA/Fe_3O_4, curcumin drug, and PLA-HA/Fe_3O_4/curcumin nanoparticles

Table 1 Analysis of variance of Ic50 of treatments value (Dunkan). **p<0.01 compared with control group.

Source of variation	*df*	MS				
		Fe_3O_4	PLA-HA	PLA-HA/Fe_3O_4	Curcumin	PLA-HA/Fe_3O_4/Curcumin
Concentration	5	66.12**	18.45**	49.66**	1047.36**	945.52**
Error	12	0.15	0.12	0.12	0.01	0.18
CV (%)	–	2.33	3.01	2.89	2.03	3.45

4 days of incubation with PBS buffer, at pH = 7.4, was 45.66 ± 2.9% (Fig. 6). Also, it was found that the drug release rate was higher in acidic pH compared to the neutral media. For example, the amount of curcumin drug released from nanoparticles in 14 days at pH = 7.4 was 59.11% ± 2.7, while this amount increased to more than 94% at pH = 6 and 98% at pH = 4.8.

3.4 In vitro cytotoxicity

MTT assay results, shown in Fig. 7, demonstrated that PLA-HA/Fe_3O_4 nanoparticles are biocompatible on HCT116 cells since the encapsulation of the drug curcumin inside these nanoparticles significantly increased its toxicity on the HCT116 cell line (Table 1). Although the encapsulation of curcumin drug inside PLA-HA/Fe_3O_4 nanoparticles increased the antitumor properties of these nanoparticles, the lowest cell viability of HCT116 cells was observed after its treatment with free curcumin drug. For example, the survival rate of cells after treatment with 200 µg/ml of PLA-HA/Fe_3O_4/curcumin nanoparticles were 58.63 ± 5.1%, while this rate was for an equal amount of curcumin drug encapsulated in 0 µg/ml of PLA-HA/Fe_3O_4/curcumin nanoparticles was 52.26 ± 4.3.

4 Discussion

In this study, PLA-HA/Fe_3O_4/curcumin nanoparticle was synthesized successfully to deliver curcumin as a drug into HCT116 Colorectal cancer cells. First, PLA-HA copolymer synthesized successfully and characterized by H-NMR, FT-IR spectra, and TGA analysis. Second, PLA-HA/Fe_3O_4/curcumin and PLA/Fe_3O_4 nanoparticles synthesized, and TEM and DLS analysis were conducted to investigate the morphological characteristics and size of nanoparticles. According to the TEM results, the synthesized PLA-HA/Fe_3O_4/curcumin nanoparticles were found to have a spherical structure. In agreement with the results obtained from the research of other researchers, it has been determined that the efficiency of drug transfer to target tissues directly depends on the morphology of nanoparticles. For example, among the types of spatial structure, nanoparticles with spherical structure have high transfer efficiency [49]. According to the results obtained in this research, due to the spherical structure, PLA-HA/Fe_3O_4/curcumin nanoparticles will have a high potential in drug delivery to cancer cells and tissues [50]. The size and surface charge of nanoparticles are two other vital factors in the successful delivery of the drug encapsulated inside the nanoparticles [51]. Following the results obtained from other research, by decreasing the size of nanoparticles, the possibility of success in transferring

them to cancer cells increases. In contrast, non-specific absorption by normal cells increases in nanoparticles with a size smaller than 50 nm [52]. In other words, by reducing the size of nanoparticles to less than 50 nm, in addition to increasing the transfer efficiency, the amount of side effects also increases with non-specific absorption by normal cells [53]. Based on the results, nanoparticles with a size of 200 nm are considered a suitable option for targeted drug delivery to cancer tissues [54]. This group of nanoparticles has a higher transfer efficiency due to their size smaller than 200 nm, and the non-specific absorption of these nanoparticles by normal cells is less than nanoparticles smaller than 100 nm. According to the results obtained in this research, the size of PLA-HA/Fe_3O_4/curcumin nanoparticles was in the range of 200 nm, so it is expected that these nanoparticles have a high penetration ability to cancer cells and minimal absorption by normal cells in vivo. In the study conducted by Noor Alaam and colleagues on designing and determining the properties of PLGA-HA nanoparticles loaded with Cisplatin, a slight increase in the size of nanoparticles conjugated with hyaluronic acid was seen compared to PLGA nanoparticles. The possible reason for this increase in size is the presence of hyaluronic acid segments. Nanoparticles containing HA in this study also had more negative zeta potential, which is due to the negative carboxylic groups present in hyaluronic acid [55].

After that, based on the obtained results of the Drug release pattern, this phenomenon is consistent with the results observed in previous studies, which have stated the biochemical mechanisms involved in the separation of drugs from nanoparticles as the probable reason for the different release rates in an acidic and neutral environment. Therefore, due to the low pH of tumor tissue compared to healthy tissue, drug release will be less in healthy cells. As a result of this process, curcumin encapsulation in synthesized nanoparticles can lead to fewer side effects [56, 57]. Many researchers are interested in using iron oxide nanoparticles in drug delivery systems because of their biocompatibility and favorable magnetic properties [58]. These nanoparticles allow drug accumulation in the tumor site by applying an external magnetic field [59]. Also, these nanoparticles have a high potential in imaging applications and hyperthermia. The results of past research have shown that magnetic nanoparticles increase the contrast of images in MRI imaging. Also, these nanoparticles significantly increase the efficiency of drug transfer to the tumor tissue [60]. In previous studies, drug release from polymer nanoparticles with a magnetic core was also examined. Amani et al. conducted a study in which, in terms of the design and evaluation of iron oxide nanoparticles coated with a PLA-PEG-PLA copolymer, the burst and continuous release patterns of drug release were observed in both neutral and acidic environments. In a similar condition, compared to a neutral medium, the rate of drug release from nanoparticles in an acidic medium was significantly higher. The chemical and biochemical processes involved in the separation of drugs from nanoparticles, as well as the reason for the difference in release rate between an acidic and a neutral environment, were discussed in this study. It was likewise expressed that, as a general rule, the course of medication partition from nanoparticles in an impartial climate is slower than in an acidic climate. When compared to healthy cells or tissues, cancer cells or tumor tissues have a lower pH, so a high rate of release in acidic tissue may result from fewer side effects than when the free drug is used [61]. In addition, polymer degradation was cited as the cause of the continuous phase release of Berberine from PLGA-HA copolymer nanoparticles in the study by Bhatnagar and colleagues. Additionally, the hydrolysis of PLGA ester bonds in an acidic environment is the cause of the faster release of Berberine than in a neutral environment. Berberine release from PLGA-HA nanoparticles was higher than that of PLGA nanoparticles in this study. Bhatnagar suggests that the increased interaction of nanoparticles with the aqueous environment is the hydrophilic nature of hyaluronic acid [62].

In this research, the PLA polymer surface was targeted by using hyaluronic acid in order to increase the efficiency of drug transfer to cancer cells. In addition, the ability to transport curcumin drug through these nanoparticles and its effect on the viability of HCT116 cells was also evaluated through the MTT test. Similar outcomes have been observed in other studies employing hyaluronic acid as a targeted component against cancer cells. Also, the findings of this research are consistent with other studies which have employed Hyaluronic acid as a tumor-targeting moiety in nanoparticles. The reason for this phenomenon could be the increased adsorption of nanoparticles by cells due to the specific interaction between hyaluronic acid present in the nanoparticle's structure and CD44 receptors, which are over-expressed on the surface of the HCT116 cell membrane. Noor Alaam's research found that when PLGA-HA nanoparticles were used instead of hyaluronic acid nanoparticles, the internalization of the nanoparticles improved because hyaluronic acid specifically interacted with CD44 receptors in SKOV-3 cells. It is excessive, and the rally is necessary for the nanoparticles' endocytosis. The cell toxicity of the drug-containing nanoparticles and the free drug was not significantly different, in contrast to the results of the current study. This is due to the ability of post-endocytosis nanoparticles to transmit drugs in more higher volumes and the cellular toxicity of the materials used in their preparation, despite the sluggishness of this process compared to the release of the free drug [55].

5 Conclusion

Chemotherapy drugs are effective at reducing cancer cell survival, although they have many side problems, such as their effect on healthy cells and resistance to the drug. In addition, due to the fast catabolism and short half-life of these drugs, continuous intravenous infusion is often used. In order to solve the obstacles mentioned above, it is possible to use drug loading in targeted nanoparticles. Encapsulation of curcumin in the magnetite (Fe_3O_4) nanoparticles prepared by green synthesis method and coated with PLA-HA copolymer could be a proper approach for addressing its non-specific effect on healthy cells. Prepared PLA-HA/Fe_3O_4/curcumin nanoparticles have a spherical shape and a size of about 200–300 nm. According to the results obtained in this research, due to the spherical structure, PLA-HA/Fe_3O_4/curcumin nanoparticles will have a high potential in drug delivery to cancer cells and tissues. The drug encapsulation efficiency in PLA-HA/Fe_3O_4 nanoparticles was $24.8 \pm 4.6\%$. The synthesized nanoparticles are able to create a two-phase release pattern explosively and continuously for 14 days. More than 50% of the drug released within three days was released. Furthermore, the amount of drug release in acidic pH is significantly higher than in neutral pH. Considering the acidity of the pH of cancer cells and tumor tissue compared to healthy tissue, this capability can lead to a decrease in the release of the drug in the healthy tissue and, as a result, reduce the side effects of the drug. Therefore, PLA-HA/Fe_3O_4/curcumin nanoparticles can be a potential approach for targeted drug delivery due to the presence of physicochemical properties and release profile, appropriate toxicity, and efficiency in transferring curcumin drug to colorectal cancer cells.

Author contributions SB led the writing of the article and proofreading of the final version of the manuscript, SA conducted the research and investigation process, MN analyzed the statistical, mathematical, and computational, and Wrote the original draft of the article, AM performed the experiments, SA provided the study materials, materials, laboratory samples, HAE supervised: oversight and leadership responsibility for the research activity planning (Correspondence) and VAH performed the numerical calculations for the suggested experiment. All authors reviewed the manuscript

Funding This study was supported by a grant from Ardabil University of Medical Sciences as a thesis No. 1005688.

Data availability The datasets generated during and/or analyzed during the current study are available from the corresponding author on reasonable request.

Declarations

Competing interests The authors declare no competing interests.

References

1. Dekker E, Tanis PJ, Vleugels J, Kasi PM, Wallace M. Pure-AMC. Lancet. 2019;394:1467–80.
2. Bando H, Ohtsu A, Yoshino T. Therapeutic landscape and future direction of metastatic colorectal cancer. Nat Rev Gastroenterol Hepatol. 2023;20(5):306–22. https://doi.org/10.1038/s41575-022-00736-1.
3. Fanotto V, Salani F, Vivaldi C, Scartozzi M, Ribero D, Puzzoni M, et al. Primary tumor resection for metastatic colorectal, gastric and pancreatic cancer patients: in search of scientific evidence to inform clinical practice. Cancers. 2023;15(3):900. https://doi.org/10.3390/cancers15030900.
4. Heemskerk-Gerritsen BA, Rookus MA, Aalfs CM, Ausems MG, Collée JM, Jansen L, et al. Improved overall survival after contralateral risk-reducing mastectomy in BRCA1/2 mutation carriers with a history of unilateral breast cancer: a prospective analysis. Int J Cancer. 2015;136(3):668–77. https://doi.org/10.1016/j.breastdis.2015.07.032.
5. Kalyan A, Kircher S, Shah H, Mulcahy M, Benson A. Updates on immunotherapy for colorectal cancer. J Gastrointest Oncol. 2018;9(1):160. https://doi.org/10.21037/jgo.2018.01.17.
6. Kircher SM, Nimeiri HS, Benson AB III. Targeting angiogenesis in colorectal cancer: tyrosine kinase inhibitors. Cancer J. 2016;22(3):182–9. https://doi.org/10.1097/ppo.0000000000000192.

7. Dasineh S, Akbarian M, Ebrahimi HA, Behbudi G. Tacrolimus-loaded chitosan-coated nanostructured lipid carriers: preparation, optimization and physicochemical characterization. Appl Nanosci. 2021;11:1169–81. https://doi.org/10.1007/s13204-021-01744-4.
8. Ebrahimi HA, Javadzadeh Y, Hamidi M, BarzegarJalali M. Development and characterization of a novel lipohydrogel nanocarrier: repaglinide as a lipophilic model drug. J Pharm Pharmacol. 2016;68(4):450–8. https://doi.org/10.1111/jphp.12537.
9. Fasili Z, Mehri F, Ebrahimi HA, Jamali Z, Mohammad Khanlou E, Kahrizi F, Salimi A. Applying nanoparticles in the treatment of viral infections and toxicological considerations. Pharm Biomed Res. 2019;5(4):1–20. https://doi.org/10.18502/pbr.v5i4.2392.
10. Willenbacher E, Khan SZ, Mujica SCA, Trapani D, Hussain S, Wolf D, et al. Curcumin: new insights into an ancient ingredient against cancer. Int J Mol Sci. 2019;20(8):1808. https://doi.org/10.3390/ijms20081808.
11. Bachmeier BE, Killian PH, Melchart D. The role of curcumin in prevention and management of metastatic disease. Int J Mol Sci. 2018;19(6):1716. https://doi.org/10.3390/ijms19061716.
12. Gonçalves PB, Romeiro NC. Multi-target natural products as alternatives against oxidative stress in chronic obstructive pulmonary disease (COPD). Eur J Med Chem. 2019;163:911–31. https://doi.org/10.1016/j.ejmech.2018.12.020.
13. Khan H, Ullah H, Nabavi SM. Mechanistic insights of hepatoprotective effects of curcumin: therapeutic updates and future prospects. Food Chem Toxicol. 2019;124:182–91. https://doi.org/10.1016/j.fct.2018.12.002.
14. Chen C-Y, Kao C-L, Liu C-M. The cancer prevention, anti-inflammatory and anti-oxidation of bioactive phytochemicals targeting the TLR4 signaling pathway. Int J Mol Sci. 2018;19(9):2729. https://doi.org/10.3390/ijms19092729.
15. Jankun J, Wyganowska-Świątkowska M, Dettlaff K, Jelińska A, Surdacka A, Wątróbska-Świetlikowska D, Skrzypczak-Jankun E. Determining whether curcumin degradation/condensation is actually bioactivation. Int J Mol Med. 2016;37(5):1151–8. https://doi.org/10.3892/ijmm.2016.2524.
16. Mirzaei H, Masoudifar A, Sahebkar A, Zare N, Sadri Nahand J, Rashidi B, et al. MicroRNA: a novel target of curcumin in cancer therapy. J Cell Physiol. 2018;233(4):3004–15. https://doi.org/10.1002/jcp.26055.
17. Bahrami A, Amerizadeh F, ShahidSales S, Khazaei M, Ghayour-Mobarhan M, Sadeghnia HR, et al. Therapeutic potential of targeting Wnt/β-catenin pathway in treatment of colorectal cancer: rational and progress. J Cell Biochem. 2017;118(8):1979–83. https://doi.org/10.1002/jcb.25903.
18. Allegra A, Innao V, Russo S, Gerace D, Alonci A, Musolino C. Anticancer activity of curcumin and its analogues: preclinical and clinical studies. Cancer Investig. 2017;35(1):1–22. https://doi.org/10.1080/07357907.2016.1247166.
19. Salehi B, Stojanović-Radić Z, Matejić J, Sharifi-Rad M, Kumar NVA, Martins N, Sharifi-Rad J. The therapeutic potential of curcumin: a review of clinical trials. Eur J Med Chem. 2019;163:527–45. https://doi.org/10.1016/j.ejmech.2018.12.016.
20. Mundekkad D, Cho WC. Applications of curcumin and its nanoforms in the treatment of cancer. Pharmaceutics. 2023;15(9):2223. https://doi.org/10.3390/pharmaceutics15092223.
21. Victorelli FD, Manni LS, Biffi S, Bortot B, Buzzá HH, Lutz-Bueno V, et al. Potential of curcumin-loaded cubosomes for topical treatment of cervical cancer. J Colloid Interface Sci. 2022;620:419–30. https://doi.org/10.1016/j.jcis.2022.04.031.
22. Tabanelli R, Brogi S, Calderone V. Improving curcumin bioavailability: current strategies and future perspectives. Pharmaceutics. 2021;13(10):1715. https://doi.org/10.3390/pharmaceutics13101715.
23. Zoi V, Galani V, Lianos GD, Voulgaris S, Kyritsis AP, Alexiou GA. The role of curcumin in cancer treatment. Biomedicines. 2021;9(9):1086. https://doi.org/10.5772/27874.
24. Pricci M, Girardi B, Giorgio F, Losurdo G, Ierardi E, Di Leo A. Curcumin and colorectal cancer: from basic to clinical evidences. Int J Mol Sci. 2020;21(7):2364. https://doi.org/10.3390/ijms21072364.
25. He Y-c, He L, Khoshaba R, Lu F-g, Cai C, Zhou F-l, et al. Curcumin nicotinate selectively induces cancer cell apoptosis and cycle arrest through a P53-mediated mechanism. Molecules. 2019;24(22):4179. https://doi.org/10.3390/molecules24224179.
26. Karthikeyan A, Senthil N, Min T. Nanocurcumin: a promising candidate for therapeutic applications. Front Pharmacol. 2020;11: 529594. https://doi.org/10.3389/fphar.2020.00487.
27. Weng W, Goel A. Curcumin and colorectal cancer: an update and current perspective on this natural medicine. Semin Cancer Biol. 2022;80:73–86. https://doi.org/10.1016/j.semcancer.2020.02.011.
28. Yusuf A, Almotairy ARZ, Henidi H, Alshehri OY, Aldughaim MS. Nanoparticles as drug delivery systems: a review of the implication of nanoparticles' physicochemical properties on responses in biological systems. Polymers. 2023;15(7):1596. https://doi.org/10.3390/polym15071596.
29. Sukumaran S, Neelakandan M, Shaji N, Prasad P, Yadunath V. Magnetic nanoparticles: synthesis and potential biological applications. JSM Nanotechnol Nanomed. 2018;6(2):1068.
30. Chen Y-T, Kolhatkar AG, Zenasni O, Xu S, Lee TR. Biosensing using magnetic particle detection techniques. Sensors. 2017;17(10):2300. https://doi.org/10.3390/s17102300.
31. Ganapathe LS, Mohamed MA, Mohamad Yunus R, Berhanuddin DD. Magnetite (Fe_3O_4) nanoparticles in biomedical application: from synthesis to surface functionalisation. Magnetochemistry. 2020;6(4):68. https://doi.org/10.3390/magnetochemistry6040068.
32. Chen Y, Ding X, Zhang Y, Natalia A, Sun X, Wang Z, Shao H. Design and synthesis of magnetic nanoparticles for biomedical diagnostics. Quant Imaging Med Surg. 2018;8(9):957. https://doi.org/10.21037/qims.2018.10.07.
33. Noqta OA, Aziz AA, Usman IA, Bououdina M. Recent advances in iron oxide nanoparticles (IONPs): synthesis and surface modification for biomedical applications. J Supercond Novel Magn. 2019;32:779–95. https://doi.org/10.1007/s10948-018-4939-6.
34. Amani A, Alizadeh MR, Yaghoubi H, Ebrahimi HA. Design and fabrication of novel multi-targeted magnetic nanoparticles for gene delivery to breast cancer cells. J Drug Deliv Sci Technol. 2021;61: 102151. https://doi.org/10.1016/j.jddst.2020.102151.
35. Nasab SH, Amani A, Ebrahimi HA, Hamidi AA. Design and preparation of a new multi-targeted drug delivery system using multifunctional nanoparticles for co-delivery of siRNA and paclitaxel. J Pharm Anal. 2021;11(2):163–73. https://doi.org/10.22541/au.157541388.85913601.
36. Drumright RE, Gruber PR, Henton DE. Polylactic acid technology. Adv Mater. 2000;12(23):1841–6.
37. Nurazzi N, Harussani M, Zulaikha NS, Norhana A, Syakir MI, Norli A. Composites based on conductive polymer with carbon nanotubes in DMMP gas sensors—an overview. Polimery. 2021;66(2):85–97. https://doi.org/10.14314/polimery.2021.2.1.

38. Ali SSS, Razman MR, Awang A. The nexus of population, GDP growth, electricity generation, electricity consumption and carbon emissions output in Malaysia. Int J Energy Econ Policy. 2020;10(3):84–9. https://doi.org/10.32479/ijeep.8987.
39. Feghali E, Tauk L, Ortiz P, Vanbroekhoven K, Eevers W. Catalytic chemical recycling of biodegradable polyesters. Polym Degrad Stab. 2020;179: 109241. https://doi.org/10.1016/j.polymdegradstab.2020.109241.
40. Amani A, Dustparast M, Noruzpour M, Zakaria RA, Ebrahimi HA. Design and invitro characterization of green synthesized magnetic nanoparticles conjugated with multitargeted poly lactic acid copolymers for co-delivery of siRNA and paclitaxel. Eur J Pharm Sci. 2021;167: 106007. https://doi.org/10.1016/j.ejps.2021.106007.
41. Maga D, Hiebel M, Aryan V. A comparative life cycle assessment of meat trays made of various packaging materials. Sustainability. 2019;11(19):5324. https://doi.org/10.3390/su11195324.
42. Chitaka TY, Russo V, von Blottnitz H. In pursuit of environmentally friendly straws: a comparative life cycle assessment of five straw material options in South Africa. Int J Life Cycle Assess. 2020;25:1818–32. https://doi.org/10.1007/s11367-020-01786-w.
43. Hajleh A, Al-Samydai A, Al-Dujaili EA. Nano, micro particulate and cosmetic delivery systems of polylactic acid: a mini review. J Cosmet Dermatol. 2020;19(11):2805–11. https://doi.org/10.1111/jocd.13696.
44. Kesharwani P, Chadar R, Sheikh A. CD44-targeted nanocarrier for cancer therapy. Front Pharmacol. 2022;12: 800481. https://doi.org/10.3389/fphar.2021.800481.
45. Ponta H, Sherman L, Herrlich PA. CD44: from adhesion molecules to signalling regulators. Nat Rev Mol Cell Biol. 2003;4(1):33–45. https://doi.org/10.1038/nrm1004.
46. Rao NV, Yoon HY, Han HS, Ko H, Son S, Lee M, et al. Recent developments in hyaluronic acid-based nanomedicine for targeted cancer treatment. Expert Opin Drug Deliv. 2016;13(2):239–52. https://doi.org/10.1517/17425247.2016.1112374.
47. Warthen J Jr, Stokes J, Jacobson M, Kozempel M. Estimation of azadirachtin content in neem extracts and formulations. J Liq Chromatogr. 1984;7(3):591–8. https://doi.org/10.1080/01483918408073988.
48. Shete P, Patil R, Tiwale B, Pawar S. Water dispersible oleic acid-coated Fe_3O_4 nanoparticles for biomedical applications. J Magn Magn Mater. 2015;377:406–10. https://doi.org/10.1016/j.jmmm.2014.10.137.
49. Bourang S, Noruzpour M, Azizi S, Yaghoubi H, Ebrahimi HA. Synthesis and *in vitro* characterization of PCL-PEG-HA/FeCo magnetic nanoparticles encapsulating curcumin and 5-FU. Nanomed J. 2024. https://doi.org/10.22038/nmj.2024.76219.1857.
50. Trang NTT, Chinh NT, Giang NV, Thanh DTM, Lam TD, Thu LV, et al. Hydrolysis of green nanocomposites of poly (lactic acid)(PLA), chitosan (CS) and polyethylene glycol (PEG) in acid solution. Green Process Synthesis. 2016;5(5):443–9. https://doi.org/10.1515/nano.0015.2016-0060.
51. Guo S, Liang Y, Liu L, Yin M, Wang A, Sun K, et al. Research on the fate of polymeric nanoparticles in the process of the intestinal absorption based on model nanoparticles with various characteristics: size, surface charge and pro-hydrophobics. J Nanobiotechnol. 2021;19:1–21. https://doi.org/10.1186/s12951-021-00770-2.
52. Chehelgerdi M, Chehelgerdi M, Allela OQB, Pecho RDC, Jayasankar N, Rao DP, et al. Progressing nanotechnology to improve targeted cancer treatment: overcoming hurdles in its clinical implementation. Mol Cancer. 2023;22(1):169. https://doi.org/10.1186/s12943-023-01865-0.
53. Shieh M-J, Peng C-L, Lou P-J, Chiu C-H, Tsai T-Y, Hsu C-Y, et al. Non-toxic phototriggered gene transfection by PAMAM-porphyrin conjugates. J Control Release. 2008;129(3):200–6. https://doi.org/10.1016/j.jconrel.2008.03.024.
54. Dang Y, Guan J. Nanoparticle-based drug delivery systems for cancer therapy. Smart Mater Med. 2020;1:10–9.
55. Alam N, Koul M, Mintoo MJ, Khare V, Gupta R, Rawat N, et al. Development and characterization of hyaluronic acid modified PLGA based nanoparticles for improved efficacy of cisplatin in solid tumor. Biomed Pharmacother. 2017;95:856–64. https://doi.org/10.1016/j.biopha.2017.08.108.
56. Bami MS, Estabragh MAR, Khazaeli P, Ohadi M, Dehghannoudeh G. pH-responsive drug delivery systems as intelligent carriers for targeted drug therapy: brief history, properties, synthesis, mechanism and application. J Drug Deliv Sci Technol. 2022;70: 102987. https://doi.org/10.1016/j.jddst.2021.102987.
57. Mahdian M, Asrari SA, Ahmadi M, Madrakian T, Jalal NR, Afkhami A, et al. Dual stimuli-responsive gelatin-based hydrogel for pH and temperature-sensitive delivery of curcumin anticancer drug. J Drug Deliv Sci Technol. 2023;84: 104537. https://doi.org/10.1016/j.jddst.2023.104537.
58. Nabavinia M, Beltran-Huarac J. Recent progress in iron oxide nanoparticles as therapeutic magnetic agents for cancer treatment and tissue engineering. ACS Appl Bio Mater. 2020;3(12):8172–87. https://doi.org/10.1021/acsabm.0c00947.
59. Monteserín M, Larumbe S, Martínez AV, Burgui S, Francisco Martín L. Recent advances in the development of magnetic nanoparticles for biomedical applications. J Nanosci Nanotechnol. 2021;21(5):2705–41.
60. Yu Q, Sun J, Zhu X, Qiu L, Xu M, Liu S, et al. Mesoporous titanium dioxide nanocarrier with magnetic-targeting and high loading efficiency for dual-modal imaging and photodynamic therapy. J Mater Chem B. 2017;5(30):6081–96. https://doi.org/10.1039/c7tb01035d.
61. Amani A, Begdelo JM, Yaghoubi H, Motallebinia S. Multifunctional magnetic nanoparticles for controlled release of anticancer drug, breast cancer cell targeting, MRI/fluorescence imaging, and anticancer drug delivery. J Drug Deliv Sci Technol. 2019;49:534–46. https://doi.org/10.1016/j.jddst.2018.12.034.
62. Bhatnagar P, Kumari M, Pahuja R, Pant A, Shukla Y, Kumar P, Gupta K. Hyaluronic acid-grafted PLGA nanoparticles for the sustained delivery of berberine chloride for an efficient suppression of Ehrlich ascites tumors. Drug Deliv Transl Res. 2018;8:565–79. https://doi.org/10.1007/s13346-018-0485-9.